Plasmid-borne *mcr-1* and Replicative Transposition of Episomal and Chromosomal blaNDM-1, blaOXA-69, and blaOXA-23 Carbapenemases in a Clinical *Acinetobacter baumannii* Isolate

Masego Mmatli[a], Nontombi Marylucy Mbelle[a], John Osei Sekyere [#ac]

[a]Department of Medical Microbiology, School of Medicine, University of Pretoria, South Africa.

[b]Department of Medical Microbiology, Tshwane Academic Division, National Health Laboratory Service, Pretoria, South Africa

[c]Department of Dermatology, School of Medicine, University of Pretoria, South Africa

[#]Address correspondence to Dr. John Osei Sekyere, Departments of Dermatology and Medical Microbiology, School of Medicine, University of Pretoria, 0084 Pretoria, South Africa: jod14139@gmail.com; j.oseisekyere@up.ac.za.

Tweet: "A clinical *A. baumannii* strain was found to possess multiple carbapenemases and an *mcr-1* colistin resistance gene on episomal chromosomes and plasmids respectively. Multiple transposition events produced multiple copies of resistance genes across the genome. This MDR strain evinces the worrying threat of untreatable infections"

Running head: *Carbapenem & colistin resistance mechanisms in K. pneumoniae*.

Abstract

Background. A multidrug-resistant clinical A. baumannii isolate with resistance to most antibiotics was isolated from a patient at an intensive care unit. The genetic environment, transcriptome, mobile, and resistome were characterized.

Method. The MicroScan system, disc diffusion, and broth microdilution were used to determine the resistance profile of the isolate. A multiplex PCR assay was also used to screen for carbapenemases and mcr-1 to -5 resistance genes. Efflux-pump inhibitors were used to evaluate efflux activity. The resistome, mobilome, epigenome, and transcriptome were characterized.

Results & conclusion. There was phenotypic resistance to 22 of the 25 antibiotics tested, intermediate resistance to levofloxacin and nalidixic acid, and susceptibility to tigecycline, which corresponded to the 27 resistance genes found in the genome, most of which occurred in multiple copies through replicative transposition. A plasmid-borne (pR-B2.MM_C3) *mcr*-1 and chromosomal bla_{PER-7}, bla_{OXA-69}, bla_{OXA-23} (three copies), bla_{ADC-25}, bla_{TEM-1B}, and bla_{NDM-1} were found within composite transposons, ISs, and/or class 1 and 2 integrons on genomic islands. Types I and II methylases and restriction endonucleases were in close synteny to these resistance genes within the genomic islands; chromosomal genomic islands aligned with known plasmids. There was a closer evolutionary relationship between the strain and global strains but not local or regional strains; the resistomes also differed. Significantly expressed/repressed genes (6.2%) included resistance genes, hypothetical proteins, mobile elements, methyltransferases, transcription factors, membrane and efflux proteins.

The genomic evolution observed in this strain explains its adaptability and pandrug resistance and shows its genomic plasticity on exposure to antibiotics.

Keywords: colistin resistance; carbapenem; carbapenemase; last-resort antibiotics; non-fermenters; multi-drug resistance; RNAseq.

1. Introduction

Acinetobacter baumannii is an aerobic, coccobacillary rod, non-fermenting Gram-negative pathogen [1,2]. It is an important, ubiquitous and opportunistic pathogen found in both moist and dry conditions and is well distributed within nature, the nosocomial environment and the human mucosal microbiome [3]. *A. baumannii* causes both community and health-care associated infections (HAIs) [4,5] including urinary tract, bloodstream, skin, and tissue, as well as ventilator-associated infections [6,7]. These infections are usually difficult to treat and are fatal [8,9] as *A. baumannii* can survive for prolonged periods in the hospital environment, facilitating its nosocomial spread [10]. This is achieved through either direct contact with an infected patient (patient-to-patient), contact with the hands of health care personnel, or indirectly by touching contaminated environmental surfaces [1,3,11]. Individuals at risk for *A. baumannii*-related HAIs are typically those who are immuno-deficient [7,10], or are undergoing invasive procedures such as the use of mechanical ventilators, central venous or urinary catheters, as seen in the invasive care unit (ICU) [4,10].

Carbapenem resistance in *A. baumannii* is mainly acquired through the production of oxacillinase-type carbapenemases, with $bla_{\text{OXA-23}}$-like and $bla_{\text{OXA-48}}$-like being the most prevalent β-lactamase (carbapenemase) [12,13]. Hence, carbapenem-resistant *A. baumannii* (CRAB) [13] is mostly treated using colistin and tigecycline as the last option. While phosphoethanolamine (PEtN)-mediated CRAB has been reported in South Africa [14,15], mobile colistin resistance (mcr) genes have been reported in *A. baumannii* in China [16], Brazil [17], Italy [18], Pakistan [7], Turkey [5], Europe 23 and Iraq 24. Nevertheless, there has been no reports of mcr-producing A. baumannii in South Africa. Hence, this study presents the first report of an *mcr*-positive CRAB isolate (with multiple carbapenemases) from South Africa and to our

knowledge, the first globally, using genomics, transcriptomics, epigenomics, and advanced bioinformatics to characterize its mechanisms of resistance and genome structure.

2. Methods

Sample source and phenotypic resistance

A 53-year-old female patient at an intensive care unit (ICU) of the Steve Biko Academic Hospital, a tertiary and quaternary hospital in Pretoria, South Africa, presented with a difficult-to-treat infection in 2017. A fluid aspirate from the patient was cultured on blood agar media for 24 hours at 37°C and subsequently identified in the laboratory; the isolate was labelled as R-B2.MM [19]. The Microscan Walkaway identification/antibiotic susceptibility testing system (Beckman Coulter Diagnostics, United States) with Panel Combo 68 was used to identify the species and antibiotic resistance profiles of the isolate. Carbapenem and colistin resistance of the isolate were confirmed using the disc diffusion (10 µg discs of ertapenem, meropenem and imipenem) and broth microdilution (BMD) methods, respectively. The Clinical Laboratory Standards Institute (CLSI) [20] and the European Committee on Antimicrobial Susceptibility Testing (EUCAST)[21] breakpoints were used respectively for the non-colistin antibiotics and colistin BMD. The BMD assay was performed using colistin sulphate powder, according to the CLSI standards.

Ertapenem sulphate salt and colistin sulphate salt (Glentham Life Sciences, United Kingdom), were used for the BMD assay [22]. *Escherichia coli* ATCC 25922 and *Pseudomonas aeruginosa* ATCC 27853 were included as quality control strains. Both antibiotics were dissolved in sterile deionized water according to the manufacturers' instructions. The antibiotic concentrations tested were: 128 µg/mL, 64 µg/mL, 32 µg/mL, 16 µg/mL, 8 µg/mL, 4 µg/mL, 2 µg/mL, 1 µg/mL, 0.5 µg/mL, and 0.25 µg/mL.

The BMD assay was performed in untreated 96-well polystyrene microtiter plates, with each well containing 100 µL of antibiotic dilution and Mueller-Hinton broth (MHB) or cation-adjusted MHB for ertapenem and colistin respectively. Subsequently, a 0.5 MacFarland suspension of bacterial culture was prepared, diluted to 1:20 with sterile saline, and 0.01 mL was inoculated into each well. The plates also included sensitive and negative control wells.

Efflux-pump inhibitors

The role of efflux pumps in the resistance mechanisms of the isolate was investigated using the BMD method and the following efflux-pump inhibitors (EPIs): verapamil, phenylalanine-arginine β-naphthylamide (PAβN), carbonyl cyanide 3-chlorophenylhydrazone (CCCP), reserpine, and ethylenediaminetetraacetic acid (EDTA). The change in carbapenem and colistin resistance minimum inhibitory concentrations (MICSs) in the presence of the EPIs were calculated. The BMD and agar plates were incubated at 37 °C for 16-18 hours, and the minimum inhibitory concentration (MIC) was determined as the lowest antibiotic concentration without visible bacterial growth; the inhibition zones (for the disc diffusion tests) were used to determine carbapenem resistance using the CLSI breakpoints [20,23]. The final concentrations of the antibiotic substrates in the broth were 1.5 µg/mL for CCCP, 4 µg/mL for VER, 25 µg/mL for PAβN, 20 µg/mL for RES, and 20 mM (pH 8.0) for EDTA. A ≥ 2-fold reduction in ertapenem and colistin MICs after EPI applications was indicative of significant efflux pump, metallo β-lactamase, and MCR activity and role in carbapenem or colistin resistance.

Molecular characterization

Genomic DNA and RNA were respectively extracted from a 24-hour culture using Quick-DNA-fungal/bacterial MiniPrep™ kit (ZymoResearch) and Quick-RNA-fungal/bacterial MiniPrep™ kit (Zymo Research) according to the manufacturer's protocols. Prior to RNA

extraction, the bacterial suspension was grown in a broth containing 0.5 mg/mL of ertapenem and 2 mg/mL of colistin for at least 12 hours. The RNA was converted into cDNA using Qiagen's cDNA synthesis kit.

Aliquots of the gDNA was used in a multiplex PCR screening test to identify the presence of *mcr* and carbapenemases using the primers in Table S1 (Dataset 1) and conditions already described in another study[19]. The gDNA was sequenced using PacBio SMRT sequencing at 100x coverage while the cDNA was sequenced using Illumina Miseq at a commercial sequencing facility. The PacBio reads (in fastQ format) were assembled using PacBio's hierarchical genome-assembly process (HGAP) software to obtain a fastA file, which was annotated with NCBIs Prokaryotic Genome Annotation Pipeline (PGAP). The methylation files (motifs and base modifications) of the genome was also obtained from PacBio's SMRTAnalysis MotifMaker software.

The species, MLST profile, resistome, mobilome, and epigenome, of the isolate were determined using NCBIs Average Nucleotide Identity (ANI) [24], Center for Genomic Epidemiology's MLST 2.0 [25], ResFinder 4.0 [26], PlasmidFinder 2.1 [27], MGE (mobile genetic element) [28], and Restriction-ModificationFinder 1.1 [29]. The GenBank annotation files were downloaded and parsed through SnapGene Version 7.2.1 to illustrate the genetic environment of the resistance genes.

Phylogenomics

A. baumannii strains that were classified as resistant by computational means or through laboratory analyses were selected from the PATRIC database. Those from Africa were separated and downloaded and those from other continents were also grouped together: a selection of 199 strains were randomly obtained from the non-African group and the genomes from the African strains were downloaded. Finally, sections of the strain's genome was

BLASTed to identify other strains that closely aligned with it. The genomes of these closely aligned strains through BLAST analysis were also downloaded for additional phylogenetic analysis. The downloaded genomes, together with this study's genome, were aligned using ClustalW and ≥1000 coding sequences were used to phylogenetically analyse their evolutionary relationship using the randomized axelerated maximum likelihood (RAxML) tool. Default parameters were used except that 1000 genes were set as the minimum for all genomes and a bootstrap of 1000 was used. The Newick file was annotated using FigTree v1.4.4.

Epigenomics

The Restriction Enzyme Database (REBASE) [29], hosted by the Centre for Epidemiology was used to identify the restriction modification system (RMS), which includes DNA methylation, restriction endonucleases, and their motifs [30]. The methylation modifications and motifs were also determined using PacBio's MotifMaker software [29]. PGAP annotations of the contigs also identified the restriction endonucleases (REs), methylases or methyltransferases (MTAses), and associated methylation genes in each contig. These annotations were visualized using SnapGene 7.2.1.

RNA-sequencing data analysis

HTSeq-DeSeq2 was used to align, assemble, and evaluate the differential gene expression of the isolate. *A. baumannii* ATCC 1909 strain was used as the reference genome. The function of each gene was evaluated using the genome annotations of the reference strain on the PATRIC database.

Data availability

This Whole Genome Shotgun project, epigenomic, and RNAseq data have been deposited at DDBJ/ENA/GenBank under the BioProject number PRJNA861833 and accession number JANIOU000000000. The version described in this paper is version JANIOU020000000.

3. Results

Identification, Typing, and Resistance Profile

The isolate was identified by the MicroScan Walkaway identification/antibiotic susceptibility testing system (Beckman Coulter Diagnostics, United States) using Panel Combo 68 as a non-fermenting, MDR and ESβL-producing isolate. The species was confirmed by NCBI's ANI [24] to be *A. baumannii*, with resistance to 22 out of the 25 antibiotics tested: amikacin, amoxicillin-clavulanate, ampicillin/sulbactam, ampicillin, aztreonam, cefepime, cefotaxime, cefoxitin, ceftazidime, cefuroxime, cephalothin, ciprofloxacin, colistin, ertapenem, fosfomycin, gentamicin, imipenem, meropenem, norfloxacin, nitrofurantoin, tobramycin, and trimethoprim-sulfamethoxazole. It was however sensitive to tigecycline and piperacillin-tazobactam, and had intermediate susceptibility to levofloxacin and nalidixic acid. The BMD and disc diffusion tests confirmed isolate R-B2.MM as resistant to both colistin (>128 µg/mL) and the carbapenems (zone diameter >19 mm).

The multiplex PCR screening of the isolate detected *mcr*-1 and a bla_{OXA}-like gene, while the whole-genome sequencing identified 27 resistance genes (or 31 resistance genes with variants): *aadA1* (six copies: three copies on chromosomal contig 1 and three copies on chromosomal contig 2), *aac(3)-Ia, aph(3)-Ia, aph(3'')-Ib, aph(6)-Id* (two copies on the chromosome; contig 1), *armA, arr-2, dfrA1* (four copies: two copies on chromosomal contig 1 and two on chromosomal contig 2), *dfrA15, mcr-1.1* (two copies on plasmid contig 3), *mphE, msrE, qacE, qnrS1, sitABCD, strA, strB, sul1* (three copies on chromosomal contig 1), *sul2* (three copies on chromosomal contig 1), *sul3, cmlA1* (two copies: one on contig 1 and

another on plasmid contig 3), *qnrS1*, *tet*(B), *tet*(M), *tet*(A) (two copies on plasmid contig 3), bla_{PER-7}, bla_{OXA-69}, bla_{OXA-23} (three copies on chromosomal contig 1), bla_{ADC-25}, bla_{TEM-1B}, and bla_{NDM-1}. The resistance phenotype corresponded to the resistome in that the resistance genes identified corresponds to the resistance profiles observed from the MicroScan and BMD (Table S3: Dataset 1).

The strain was found to belong to multilocus sequence types (MLSTs) ST1604, ST231, or ST1: ST1604 and ST231 from the Oxford MLST scheme and ST1 according to the Pasteur MLST Scheme. This strain contained 12 virulence genes: cma, ompT, traT, iutA, iucC, iss, hlyF, iroN, sitA, cib, cvaC, and ipfA.

Among the four EPIs, EDTA (71.3-fold change) and CCCP (2.5-fold change) had a significant MIC reduction (≥ 2-fold) on colistin while the rest did not. Notably, the *P. aeruginosa* ATCC 27853 had a significant reduction in colistin MIC in the presence of EDTA (2-fold reduction) and reserpine (4.7-fold reduction). Contrarily, only EDTA caused a reduction (22.7-fold) in the MIC of ertapenem while PAβN and CCCP significantly reduced the MICs of ertapenem by 2-fold in the *E. coli* ATCC 25922.

Genetic environment of resistance genes

Contigs 1 and 2 were chromosomal, with contig 1 containing more resistance genes than contig 2. Notably, contigs 1 and 2 also had their resistance genes being clustered together in one region flanked by integron cassettes and composite transposons, forming a genomic island. On contig 1, the resistance genes clustered between 0 – 80 kb within integrases, recombinases, insertion sequences, transposons, DNA (cytosine) methyltransferases and methylases (Fig. S1-S5). Hence, all the resistance genes within this ~80kb genomic island were bracketed by composite transposons that also included class1 and class 2 gene cassettes. Within the genomic island on contig 1, *aadA*, *sat2*, and *dfrA1* were contiguous to each other

and bracketed by Tns*D* and *IS*256 transposases. *Aph(6')-I* was flanked by a class 2 integrase (*IntI2*) and IS*Vsa3* transposase, followed in close synteny by *sul2*, N-6 DNA methylase, IS*26*, and class 1 integrase (*IntI1*) in the reverse orientation to the *IntI*2. Following this *IntI1* integron cassette were batteries of *IS*s, transposases, and resistance genes such as *arr-2*, *cmlA5*, *QacE*, *sul1*, bla_{PER}, *sul1*, *armA*, *msr(E)*, *mph(E)*, *tetR(B)*, and *sul2*. Instructively, there were two copies of *sul1* and *sul2* genes within the genomic island (Fig. S2-S3).

Indeed, the whole genomic island of ~80kb seems to be a composite transposon and an episome as a BLAST analysis showed that it aligned with several plasmids such as Ab04-mff plasmid pAB04-1 (CP012007.1) and chromosomes such as that of *A. baumannii* AR_0083 (CP027528.1). Moreover, replicative transposition was observed at 1.19 – 1.22Mb, 1.23 – 1.28Mb, and 1.32 – 1.33Mb regions on contig 1 (Fig. 1 and 2A) with bla_{OXA-23} flanked by a type IIL restriction-modification enzyme *Mme*I and two IS*Aba1* transposases at both sides, forming a composite transposon. In Figure 1A, additional Tn*SA*, Tn*iB*, Tn*iQ* and Mu transposases were in close proximity to the composite IS*Aba1*-flanked transposases while a homocysteine S-methyltransferase was found in close proximity to the same composite transposon in Figure 1B. Thus, three copies of bla_{OXA-23} within an IS*Aba1*-flanked composite transposon were present in the genome owing to this replicative transposition. These three copies ranged from 1.19 – 1.34 Mb (Fig. 1 & 2A), which aligned to both chromosomes (including that of *A. baumannii* AR_0083 (CP027528.1)) and to an unnamed1 plasmid (90% query cover and 97.7% nucleotide identity) from *A. baumannii* 2021CK-01407 (CP104448.1) when BLASTed.

Another genomic island with a composite transposon flanking *aph(3")-Ib*, *aph(6)-Id*, bla_{NDM-1}:*ble*, and *sul2* was found between 328 – 353kb on contig 1, which aligned to both *A. baumannii* plasmids and chromosomes: CP027528.1, AP031576.1, CP130627.1, CP035935.1, CP090865.1. The composite transposon comprised of IS*1006*, recombinase,

IS*Aba1*, IS*30*, IS*91*, and IS*Vsa3* with IS*30:bla*$_{NDM-1}$*:ble* synteny being present (Fig. 2B). A third genomic island was also identified on contig 1 between 455kb and 500kb (Fig. 3A), which comprised of a class 1 integron (*IntI1*), a recombinase, DNA adenine methylase, IS*Ppu12* and IS*26*-IS*6* transposases, and *aph(3')-Ia*, GNAT N-acetyltransferase (2 copies), *aadA1, QacEΔ1, aac(3')-Ia, aadA1*, and *sul1* resistance genes. This genomic island was in close synteny with an upstream *par*C gene and mostly aligned with chromosomes and a single plasmid (from *A. baumannii* 2021CK-01407 (CP104448.1) when BLASTed (Fig. 3A).

Between 135-250kb on contig 1, methyltransferases, IS*Aba1* transposase and *gyr*B were found, without any other resistance gene (Fig. S4-S5). A *bla*$_{OXA-51}$ carbapenemase gene, in close synteny with an N-acetyltransferase and a *trmA* methylase was found within 2.04 – 2.06 Mbp on contig 1 without any MGE (Fig. 3B). Towards the end of contig 1 (2.375Mbp – end), however, *dfrA1, sat2*, and *aadA1* were bracketed by an *IntI2* class 1 integron, IS*256*, Tn*7*-like (Tn*sE*-Tn*SD*) and a truncated transposase (Fig. 3C). A BLAST analysis of this region showed that it aligned with only chromosomes from both *A. baumannii* and other Enterobacterales species such as *Proteus mirabilis, Enterobacter hormaechei, Shigella sonnei, Citrobacter freundii/gillenii, Providencia rettgeri, Morganella morganii, Escherichia coli,* and *Moellerella wisconsensis*.

Figure 4 shows the resistance genes and their genetic environments on contig 2. Notably, the beginning (0 – 15kb; Fig. 2A) and end (1.8Mb – end; Fig. 2C) of this contig has the same resistance genes and MGEs but in opposite directions/orientations: *dfrA:sat2:aadA:::*IS*26:Tn7*-Ts*E:*Tn*7*-Ts*D::integrase/recombinase:*Tn*SA* endonuclease in the 5'-3' direction and Tn*SA* endonuclease:integrase/recombinase::Tn*7*-Ts*D*:Tn*7*-Ts*E*:IS*26*:::*aadA:sat2:dfrA* in the 3'-5' direction. Between these two repeated regions, ~714 – 716kb, is the *bla*$_{ADC}$*:*IS*Aba1*resistance gene and IS (Fig. 4B). A BLAST analysis of the two

repeated regions shown in Figures 2A and 2C showed that both regions aligned to chromosomes of *A. baumannii* and other Enterobacterales species.

R-B2.MM had two plasmids, contigs 3 (pR-B2.MM_C3) and 5 (pR-B2.MM_C6), identified through BLAST analyses of the contig sequences and found to be circular. While the plasmid type for pR-B2.MM_C6 was not identifiable, with only a repM replicase gene found on it, pR-B2.MM_C3 was found to contain IncFIB, IncX1 and IncFIC(FII) replicase gene sequences (Fig. 5, S6-S7). Indeed, the pR-B2.MM_C6 plasmid had 100% coverage and nucleotide identity to *A. baumannii* plasmids such as CP145435.1 and CP142898.1 (Fig. S7) while pR-B2.MM_C3 plasmid had 65-77% coverage and 99% nucleotide identity with *E. coli* and *K. pneumoniae* plasmids (Fig. S6; Dataset 1: Table S3). The BLAST analyses of pR-B2.MM_C6 shows that the plasmids it aligned 100% to were more than 17462 bp long while pR-B2.MM_C6 was 8731bp with 11 protein genes. pR-B2.MM_C3 was 193,714bp with 184 protein-coding genes and only aligned with high nucleotide homology (99%) with sections of *E. coli* and *K. pneumoniae* plasmids (Fig. 5, S6; Dataset 1: Table S3).

AadA1, *bla*$_{TEM-1B}$, *mcr-1*, *cmlA1*, *qnrS1*, *sul3*, *tet(M)*, *tet(A)*, and *dfrA* were found on pR-B2.MM_C3 while pR-B2.MM_C6 had no resistance gene. The resistance genes on pR-B2.MM_C3 were localized together in a genomic island (between 0 - 42kb and 155 - 0kb) (Fig. 5 & S6) with *mcr-1* being flanked by IS*Apl1* and IS*903B* transposase. *Tet*(M) and the other resistance genes on this plasmid were also flanked by a class-1 integron and recombinase, which were also bracketed by batteries of Tn*3* composite transposons and insertion sequences (ISs) (Fig. 5A & 5C). Within this genomic island were site-specific MTAses and restriction endonucleases (REs) (Fig. 5; S6). Although mobile genetic elements

(MGEs) such as IS*1A*, IS*IB*, and IS*3* were also found within the 90kb – 150kb region, only an Mig-14 resistance gene was found in this region (Fig. 5B).

Phylogenomic analysis

The strain was not significantly related to any of the antibiotic-resistant strains from Africa used in the phylogenomic analysis (Fig. 6). It was closely related to two strains (with a bootstrap value of 5): *A. baumannii* 13367 and 13259. Expectedly, these two strains had different STs from each other and from R-B2.MM. There was also little uniformity in their resistomes, with *A. baumannii* 13367 having more similarity to R-B2.MM's resistome (Fig. 6). Among the global *A. baumannii* strains, however, there were significant evolutionary relationship between A. baumannii strains Ab905, Ab241, Ab238, A3232, and AbCTX19 (Fig. 7) as confirmed by the high bootstrap value of 100. *A. baumannii* Ab905 and Ab241 strains isolated from blood from Israel had the same resistome, but the remaining strains had similar but not the same resistome. Notably, bla_{ADC}, $bla_{OXA\text{-}71/69}$, $bla_{OXA\text{-}23}$, *sul1*, and *gyrA* S81L mutation was common among most of the strains. *A. baumannii* strains A3232 (Greece), AbCTX19 (France), and R-B2.MM had the same ST and belonged to the same clone.

A. baumannii strains that aligned closely with this study's strain, with more than 80% nucleotide homology and 70% query length with sections of R-B2.MM genome, were used to conduct a phylogenomic reconstruction analysis. As shown in Figure S9 (Dataset 2), 33 strains had very close evolutionary relationship with this study's strain, most of which was of ST231 or ST1 clone. Although these strains were isolated from different sources, different years, and different countries, they were closely related to each other. However, the resistome was not conserved across these strains.

Epigenomics

REBASE identified types I (M.Aca7364II and M.Aba0083I) and II (M.Aba858II) methyltransferases (MTAses), with types III and IV being absent: both types were found on only contig 1 (chromosome). A specificity subunit (S.Aba0083I) was also found on contig 1 (Dataset 4). The recognition sequence of these REs were different except for only M.Aba0083I and S.Aba0083I. GATC motif was identified by PacBio with N6-methyladenosine (m6A) modifications (Dataset 4). Type IIL restriction modification enzyme MmeI, homocysteine S-methyltransferase family protein (Fig. 1-2), Tr*mA* and DNA adenine methylase (Fig. 3), Tns*A* endonuclease (Fig. 4), and site-specific DNA-methyltransferase and RE on pR-B2.MM_C3 contig 3 (Fig. 5) were annotated throughout the genome. The annotated MTAses and REs were mostly associated with the MGEs within the composite transposons or flanked by ISs.

Differentially Expressed Genes

The fold changes of each coding gene's expression levels are shown in supplementary dataset 3. Out of the 4220 coding genes, 261 were significantly expressed while 3959 were not significantly expressed. As show in the volcano plot in Figure 8 and in the summarised bar chart in Figure S8, most of the significantly expressed genes were hypothetical proteins with unknown functions, followed by LysR family transcriptional regulators, phage replication proteins, class A beta-lactamases, GNAT resistance genes, outer membrane proteins, type I RMS, integrases, ABC/MFS efflux transporters, type-6 secretion systems (TSSS), OprD porins, etc. There were also MTAses, endonuclease III, MGEs, ABC/RND transporters, and prophages that were not significantly expressed (Dataset 3). Notably, the following resistance genes were significantly highly expressed: bla_{NDM}, *QacE*, *sul2*, recombinase, aminoglycoside 3'-phosphotransferase, *aph(3')-III/aph(3')-IV/aph(3')-VI/aph(3')-VII*, aminoglycoside 3''-phosphotransferase, *aph(3'')-I*, macrolide 2'-phosphotransferase *mph(E)/mph(G)* family, and a class A beta-lactamase.

4. Discussion

We report on the transcriptome, resistome, mobilome, epigenome and evolutionary biology of a pandrug-resistant *A. baumannii* clinical strain that harboured NDM, OXA-23, OXA-69, ADC, MCR-1, and a plethora of resistance genes. To our knowledge, this is the first CRAB strain to co-harbour three carbapenemases i.e., NDM, OXA-23, and OXA-69, and an MCR-1 globally [19,31], with the *mcr*-1 being found on a plasmid. Although NDM and OXA-23 were not found on plasmids, they were found within composite transposons within sections of the chromosome that aligned with plasmids, suggesting that they might have been integrated into the chromosomes from plasmids to form episomes. This suspicion is confirmed by the replicative transposition of the composite transposon genomic islands to other loci of the genome to form multiple genomic copies of the same genes or composite transposons (Fig. 1-4). It is further corroborated by the alignment of these genomic islands to Enterobacterales species such as *E. coli*, *K. pneumoniae*, *Serratia sp.*, *Providencia sp.*, etc. Indeed, *mcr-1* was also found within a composite transposon genomic island that can also be transposed from the plasmid to the chromosome (Fig. 5).

We are therefore of the opinion that this strain's genome underwent multiple replicative transposition events mediated by the composite transposons, recombinases and integrons that blanketed the resistance genes, resulting in the duplication of resistance genes across the genome. The strain's chromosome also contains several plasmid-integrated regions or resistance genomic islands, forming episomes that also aligns to other Enterobacterales species and plasmids. The evolutionary biology and phylogenetic analysis of the strain, as well as the comparative resistome analysis with other closely related strains and clones show that the resistome of our strain is quite unique (Fig. 6-7; S9). Hence, it is obvious that the genomic rearrangements observed in this genome is not wholly vertically transferred although it can vertically transfer this genome to other daughter cells as it multiplies. It can

also easily transfer these resistance genomic islands horizontally to other cells through the multiple MGEs such as IS, transposons, recombinases, integrases, and plasmids found in the genome (Fig. S1-S7; Fig. 1-5).

Instructively, there was no strain from South Africa and Africa, published to date, that was closely related to this study's strain while international strains were found to be within the same clade and of the same clone as this study's strain (Fig. 6-7; S9). This suggests that this strain might have been imported from abroad. Notably, the other international strains that were found to be of the same clone and clade as R-B2.MM were isolated from different clinical sources such as blood, wound, urine, respiratory specimen, rectal swabs, and fluid aspirates, from different time periods spanning 1982 to 2023, and from different countries located across all continents: South and North America, Asia and the Middle East, Europe, and Australia. While this speaks to the wide geographical distribution of these strains and clade, and portend the worrying spread of MDR *A. baumannii* strains, their non-uniform resistome is also revealing. As discussed in the previous paragraph, the non-homogeneity of resistomes across the clade shows independent evolution of resistance traits as the strains spread across the globe.

The intra-genomic evolution seen in our strain, therefore, suggests that its exposure to antibiotics during treatment might have induced the replicative transposition events observed in the genome. This further supports the need to be measured in antibiotic administration to reign in the evolution and dissemination of antibiotic resistance within and across strains and species. Indeed, the transcriptomic data lends further evidence to this assertion in that we observed significant hyperexpression of genes involved in antibiotic resistance, including resistance genes, MGEs, MTAses, REs, transcription factors, membrane-associated proteins, T6SS, phage-associated genes, etc. (Dataset 3). Evidently, the exposure to antibiotics do not only cause an increase in resistance genes expression, but also in selected efflux pumps,

386 regulatory genes, and MGEs that can both help the cell to survive by expelling xenobiotics as
387 well as adapt its genome through accelerated transposition and transcription events to confer
388 resistance.

389 This argument is supported by the presence of RMS (MTAses and REs) within the resistance
390 genomic islands or in close synteny to the composite transposons. Given the important
391 regulatory role of RMS in initiating or inhibiting transcription of key genes through DNA
392 methylation, it is evident that its close association with the MGEs and its significant
393 expression support its involvement in the observed transposition events and resistance. It has
394 already been proven that exposure to low dose antibiotics, which lead to antibiotic-resistance
395 mutations and adaptations, are mediated epigenetically through the RMS [32,33]. Hence, the
396 unique genomic arrangements and MGEs found in this isolate, which makes it different from
397 other clones within the same clade, could most likely be mediated epigenetically. Adaptive
398 resistance, which is mediated by epigenetic RMS factors, is transient nature and tends to
399 disappear in the absence of the triggering factor. This further supports our assertion that this
400 strain independently developed its MGE-mediated genomic evolution from antibiotic therapy
401 using the epigenetic RMS pathways to regulate transcription of key genes [32,33].

402 Phenotypically, not all the EPIs resulted in a reduction in MICs of both ertapenem and
403 colistin. Whereas EDTA and CCCP reduced colistin's MIC, EDTA alone could reduce the
404 MIC of ertapenem. This is expected as NDM and MCR-1 are zinc-based metallo-β-
405 lactamases, meaning that NDM and MCR-1 cannot function enzymatically without zinc [34].
406 Hence, the ability of EDTA to chelate zinc will prevent NDM and MCR-1 from being able to
407 respectively hydrolyse their substrate antibiotics or transfer a phosphoethanolamine (PEtN)
408 residue to lipid A in the outer membrane [35,36]. The ability of CCCP, on the other hand, to
409 inhibit colistin resistance is believed to be due to its ability to depolarize the plasma
410 membrane and reduce ATP production [35]. As colistin depolarizes the cell membrane, making

it more permeable to leakages, CCCP seems to work in synergy with colistin. Hence, in the presence of CCCP, MCR-1 may be unable to counter the effect of colistin by adding PEtN to lipid A [35]. Furthermore, the inability of the other EPIs to reduce ertapenem and colistin resistance was confirmed by the transcriptomic data in which many efflux pumps were not significantly expressed. Reserpine is also known to mainly inhibit major facilitator superfamily (MFS)-type efflux pumps in Gram-positive bacteria [37]. Hence, its inability to affect the MICs is expected. Verapamil and PAβN are respectively known to target MATE and RND pumps in Gram-negative bacteria [37]. However, there was no significant expression of the MFS, MATE, and RND efflux pumps from the transcriptomic data, which explains why these EPIs did not have any effect on the MICs (Dataset 3).

The repertoire of resistance genes found within the genomes correlated with the resistance phenome observed in the strain, showing that the resistance genes were being expressed to confer resistance to their respective antibiotic targets. This was also confirmed by the transcriptomic data with regards to the efflux, membrane protein and resistance genes hyperexpression (Dataset 3). Further, the association of these resistance genes on gene cassettes or within the composite transposon shows that they are moved together with the MCR-1 and carbapenemases during the transposition events or horizontal gene transfer. Hence, it is expected that this pandrug-resistant strain can share its rich resistome with other commensals or pathogens within the same niche. This will become particularly so should such a population become exposed to antibiotics, which can trigger the epigenomic and transcriptional activity towards a resistant phenotype [32,33]. One major limitation of this study was our inability to undertake a plasmid conjugation experiment to determine the transferability of the plasmid found in this strain. Yet, the clone of R-B2.MM, ST1/ST231, is found worldwide, according to the PubMLST database, in humans with a single case, ST1/ST231, collected from the environment in Croatia. All three sequence types have been

436 reported in Africa, specifically Ethiopia, Kenya and Ghana and, only ST1 has been
437 previously reported in South Africa (Pretoria) in 2010 [38].

438 The immediate genetic environment of the ARGs corroborated what has already been
439 reported globally. For instance, *mcr-1* was flanked by IS*Apl1; tet*(A) and *tet*(M) by an
440 IS*6*/IS*26*-Tn*3; sul* and *dfrA* by a class-1 integron-IS*26; bla*$_{NDM}$:*ble, aph(6')-Id* and *aph(3")-*
441 *Ib* by IS*Aba1-IS*91-*ISIS*30; *bla*$_{OXA-23}$ by IS-4-like IS*Aba1; and aadA1, qacE* and *sul1* by
442 *Inti1*-IS*6* [31,39]. The *mcr-1* was found on an IncF-IncX hybrid plasmid while most *mcr-1* genes
443 are found on IncH and IncC [31,40].

444 The absence of Types III and IV RMSs is confirmed by other studies [30,31]. Most of the REs
445 and MTAses were found on the chromosomes[30] within the genomic islands or in very close
446 synteny to the ARGs. However, not all the MTASes and REs were hyper-expressed
447 significantly (Dataset 4), suggesting that only a few of the epigenomic factors were triggered
448 by the exposure to antibiotics. There were no orphan MTAses as REs were found on both the
449 plasmid and chromosome alongside the MTAses within the genomic islands. This contrasts
450 with other studies that found several orphan MTAses (without corresponding REs) [30,41]. No
451 cytosine methyltransferase (Dcm) was found in the genome, meaning that cytosine is not
452 methylated but adenine (Dam) is methylated at the G**A**TC motif, resulting in a methylated
453 adenine at the N6 position (m6A or ^{6m}A). The G**A**TC M6A motif is ubiquitous among
454 prokaryotes [30,31,41].

455 Whereas some MTAses and REs were upregulated, some were not, suggesting that not all the
456 RMSs were triggered by exposure to antibiotics. However, the functional summary of the
457 differentially expressed genes shows that there are several unknown proteins that are
458 marshalled in the face of antibiotics exposure to protect the bacterial cell from death. The
459 significant differentially expressed genes (DEGs) with known functions included phage

proteins and MGEs, outer membrane and efflux proteins, regulatory proteins and transcription factors, lipoproteins (useful for cell membrane structures), type-6 secretion systems, and ARGs. Instructively, eighty-five genes were upregulated while 176 were downregulated, resulting in 261 DEGs, indicating that a smaller fraction of the cellular machinery (6.2%) were marshalled to deal with the antibiotic threat. None of the RNAs in the genome was significantly expressed, which could be because colistin does not attack the RNA. Yet, it is intriguing that no RNA was hyper-expressed to produce more proteins.

Conclusion

R-B2.MM encodes 35 resistance genes and twelve virulence genes, two plasmids (one of which is a hybrid IncX-IncF plasmid), and an MGE-rich chromosome with multiple resistance genomic islands that are episomal and aligns with plasmids and other Enterobacterales species. The strain was of closer evolutionary distance to several international strains suggesting that it was imported into South Africa. However, its resistome was unique, suggesting an independent evolution on exposure to antibiotic therapy mediated by epigenomic factors and MGE transposition events. The varied mechanisms available to this strain to overcome antibiotic resistance and spread to other areas and/or share its resistance determinants is worrying. This is ultimately a risk to public health as it was susceptible to only tigecycline. There is no better argument for antibiotic stewardship than the evidence provided herein to safeguard public health.

Funding: This work was funded by a grant from the National Health Laboratory Service (NHLS) given to Dr. John Osei Sekyere under grant number GRANT004 94809 (reference number PR2010486).

Acknowledgements: This work is based on the research supported wholly/in part by the National Research Foundation of South Africa under grant number: 131013. We are grateful to Dr. Busisiwe Lebogang Skosana for her assistance with the isolates' collection.

Transparency declaration: None

Conflict of interest: The authors have no conflicts of interest to declare. All co-authors have seen and agree with the contents of the manuscript.

Author contributions: MM undertook laboratory work; NMM was a co-supervisor to the study and assisted with funding; JOS designed and supervised the study, undertook data and bioinformatic analyses and visualizations, wrote and reviewed the manuscript.

5. References

1. Weber, D. J., Rutala, W. A., Miller, M. B., Huslage, K. & Sickbert-Bennett, E. Role of hospital surfaces in the transmission of emerging health care-associated pathogens: norovirus, Clostridium difficile, and Acinetobacter species. *Am. J. Infect. Control* **38**, S25-33 (2010).

2. Munoz-Price, L. S. & Weinstein, R. A. Acinetobacter infection. *N. Engl. J. Med.* **358**, 1271–1281 (2008).

3. Anane A, Y., Apalata, T., Vasaikar, S., Okuthe, G. E. & Songca, S. Prevalence and molecular analysis of multidrug-resistant Acinetobacter baumannii in the extra-hospital environment in Mthatha, South Africa. *Braz. J. Infect. Dis.* **23**, 371–380 (2019).

4. Fournier, P. E. & Richet, H. The epidemiology and control of Acinetobacter baumannii in health care facilities. *Clin. Infect. Dis.* **42**, 692–699 (2006).

5. Ghaffoori Kanaan, M. H., Al-Shadeedi, S. M. J., Al-Massody, A. J. & Ghasemian, A. Drug resistance and virulence traits of Acinetobacter baumannii from Turkey and chicken raw meat. *Comp. Immunol. Microbiol. Infect. Dis.* **70**, 101451 (2020).

6. Coyne, S., Courvalin, P. & Périchon, B. Efflux-mediated antibiotic resistance in Acinetobacter spp. *Antimicrob. Agents Chemother.* **55**, 947–953 (2011).

7. Hameed, F. *et al.* Plasmid-mediated mcr-1 gene in Acinetobacter baumannii and Pseudomonas aeruginosa: first report from Pakistan. *Rev. Soc. Bras. Med. Trop.* **52**, e20190237 (2019).

8. Maasdorp, S. D., Potgieter, S., Glover, E. & Joubert, G. Treatment outcomes of Acinetobacter baumannii -associated pneumonia and/or bacteraemia at the intensive care unit of Universitas Academic Hospital, Bloemfontein, South Africa. *African J. Thorac. Crit. care Med.* **27**, 14–17 (2021).

9. Osei Sekyere, J. & Reta, M. A. Genomic and Resistance Epidemiology of Gram-Negative Bacteria in Africa: a Systematic Review and Phylogenomic Analyses from a One Health Perspective. *mSystems* **5**, (2020).

10. Ahmed, N. H., Baba, K., Clay, C., Lekalakala, R. & Hoosen, A. A. In vitro activity of tigecycline against clinical isolates of carbapenem resistant Acinetobacter baumannii

complex in Pretoria, South Africa. *BMC Res. Notes* **5**, 215 (2012).

11. Markogiannakis, A. *et al.* Cross-transmission of multidrug-resistant Acinetobacter baumannii clonal strains causing episodes of sepsis in a trauma intensive care unit. *Infect. Control Hosp. Epidemiol.* **29**, 410–417 (2008).

12. Anane, Y. A., Apalata, T., Vasaikar, S., Okuthe, G. E. & Songca, S. Molecular Detection of Carbapenemase-Encoding Genes in Multidrug-Resistant Acinetobacter baumannii Clinical Isolates in South Africa. *Int. J. Microbiol.* **2020**, 7380740 (2020).

13. Lowe, M. *et al.* Acinetobacter baumannii: Epidemiological and Beta-Lactamase Data From Two Tertiary Academic Hospitals in Tshwane, South Africa. *Front. Microbiol.* **9**, 1280 (2018).

14. Snyman, Y. *et al.* Clonal expansion of colistin-resistant Acinetobacter baumannii isolates in Cape Town, South Africa. *Int. J. Infect. Dis.* **91**, 94–100 (2020).

15. Trebosc, V. *et al.* Dissecting Colistin Resistance Mechanisms in Extensively Drug-Resistant Acinetobacter baumannii Clinical Isolates. *MBio* **10**, (2019).

16. Ma, F. *et al.* Identification of a Novel Plasmid Carrying mcr-4.3 in an Acinetobacter baumannii Strain in China. *Antimicrob. Agents Chemother.* **63**, (2019).

17. Martins-Sorenson, N. *et al.* A novel plasmid-encoded mcr-4.3 gene in a colistin-resistant Acinetobacter baumannii clinical strain. *J. Antimicrob. Chemother.* **75**, 60–64 (2020).

18. Caselli, E., D'Accolti, M., Soffritti, I., Piffanelli, M. & Mazzacane, S. Spread of *mcr-1* –Driven Colistin Resistance on Hospital Surfaces, Italy. *Emerg. Infect. Dis.* **24**, (2018).

19. Mmatli, M., Leshaba, T. M. S., Skosana, L. B., Mbelle, N. M. & Osei Sekyere, J. Molecular Screening of Clinical Multidrug-Resistant Gram-Negative Bacteria Shows Endemicity of Carbapenemases, Coexistence of Multiple Carbapenemases, and Rarity of mcr in South Africa. *Microb. Drug Resist.* **28**, 1028–1036 (2022).

20. CLSI & Clinical and Laboratory Standards Institute (CLSI). *Performance standards for Antimicrobial Susceptibility Testing; Twenty-Seventh Informational Supplement M100-ED33:2023*. https://clsi.org/standards/products/microbiology/documents/m100/ (2023).

21. European Committee on Antimicrobial Susceptibility Testing, (EUCAST). *Breakpoint tables for interpretations of MICs and zone diameters. Version 14.0. Enterobacteriaceae* (EUCAST, 2024).

22. Al-Kadmy, I. M. S. S. *et al.* Prevalence of Genes Involved in Colistin Resistance in Acinetobacter baumannii: First Report from Iraq. *Microb. Drug Resist.* **26**, 616–622 (2019).

23. Caselli, E., D'Accolti, M., Soffritti, I., Piffanelli, M. & Mazzacane, S. Spread of mcr-1-Driven Colistin Resistance on Hospital Surfaces, Italy. *Emerg. Infect. Dis.* **24**, 1752–1753 (2018).

24. NCBI. Using Average Nucleotide Identity (ANI) to Expose Potentially Problematic Taxonomic Merges - NCBI Insights. *NCBI Insights* (2023).

25. Larsen, M. V. *et al.* Multilocus Sequence Typing of Total-Genome-Sequenced

Bacteria. *J. Clin. Microbiol.* **50**, 1355–1361 (2012).

26. Bortolaia, V. *et al.* ResFinder 4.0 for predictions of phenotypes from genotypes. *J. Antimicrob. Chemother.* **75**, 3491–3500 (2020).

27. Clausen, P. T. L. C., Aarestrup, F. M. & Lund, O. Rapid and precise alignment of raw reads against redundant databases with KMA. *BMC Bioinformatics* **19**, (2018).

28. Johansson, M. H. K. *et al.* Detection of mobile genetic elements associated with antibiotic resistance in Salmonella enterica using a newly developed web tool: MobileElementFinder. *J. Antimicrob. Chemother.* **76**, 101–109 (2021).

29. Roer, L. *et al.* Is the Evolution of Salmonella enterica subsp. enterica Linked to Restriction-Modification Systems? *mSystems* **1**, (2016).

30. Kopotsa, K., Mbelle, N. M., Sekyere, J. O. & Osei Sekyere, J. Epigenomics, genomics, resistome, mobilome, virulome and evolutionary phylogenomics of carbapenem-resistant Klebsiella pneumoniae clinical strains. *Microb. Genomics* **6**, 2020.06.20.20135632 (2020).

31. Ramaloko, W. T. & Osei Sekyere, J. Phylogenomics, epigenomics, virulome and mobilome of Gram-negative bacteria co-resistant to carbapenems and polymyxins: a One Health systematic review and meta-analyses. *Environ. Microbiol.* **24**, 1518–1542 (2022).

32. Crimi, E. *et al.* Clinical epigenetics and multidrug-resistant bacterial infections: host remodelling in critical illness. *Epigenetics* **15**, 1021–1034 (2020).

33. D'Aquila, P., De Rango, F., Paparazzo, E., Passarino, G. & Bellizzi, D. Epigenetic-Based Regulation of Transcriptome in Escherichia coli Adaptive Antibiotic Resistance. *Microbiol. Spectr.* **11**, (2023).

34. Leshaba, T. M. S., Mbelle, N. M. & Osei Sekyere, J. Current and emerging polymyxin resistance diagnostics: a systematic review of established and novel detection methods. *J. Appl. Microbiol.* jam.15184 (2021) doi:10.1111/jam.15184.

35. Osei Sekyere, J. & Amoako, D. G. Genomic and Phenotypic Characterisation of Fluoroquinolone Resistance Mechanisms in Enterobacteriaceae in Durban, South Africa. *PLoS One* **12**, 1–14 (2017).

36. Mmatli, M., Mbelle, N. M., Maningi, N. E. & Osei Sekyere, J. Emerging Transcriptional and Genomic Mechanisms Mediating Carbapenem and Polymyxin Resistance in Enterobacteriaceae : a Systematic Review of Current Reports. *mSystems* **5**, (2020).

37. Sharma, A., Gupta, V. K. & Pathania, R. Efflux pump inhibitors for bacterial pathogens: From bench to bedside. *Indian J. Med. Res.* **149**, 129 (2019).

38. Jolley, K. A., Bray, J. E. & Maiden, M. C. J. Open-access bacterial population genomics: BIGSdb software, the PubMLST.org website and their applications. *Wellcome Open Res.* **3**, (2018).

39. Partridge, S. R., Kwong, S. M., Firth, N. & Jensen, S. O. Mobile Genetic Elements Associated with Antimicrobial Resistance. *Clin. Microbiol. Rev.* **31**, 1–61 (2018).

40. Mmatli, M., Mbelle, N. M. & Osei Sekyere, J. Global epidemiology, genetic

environment, risk factors and therapeutic prospects of mcr genes: A current and emerging update. *Front. Cell. Infect. Microbiol.* **12**, (2022).

41. Blow, M. J. *et al.* The Epigenomic Landscape of Prokaryotes. *PLoS Genet.* **12**, e1005854 (2016).

Figures

Figure 1. Genetic environment of blaOXA-23 carbapenemase on chromosomal contig 1 (1.19-1.22Mb, 1.23-1.28Mb). Mobile genetic elements (shown as red arrows) and methylases/restriction modification endonuclease (purple arrows) bracketing the bla_{OXA-23} gene shows that the gene is within a composite transposon. The same chromosomal contig has two bla_{OXA-23} genes shown in A and B, with the genetic environment in A being different from that in B. In both cases, bla_{OXA-23} was bracketed by IS*Aba1* and transposases.

Figure 2. Genetic environment of sul2, aph(3")lb, aph(6)-ld, and blaOXA-23 and blaNDM-1 carbapenemase on chromosomal contig 1 (~1.32-1.34Mb, ~320-360kb). bla_{OXA-23} (shown as blue arrow) in A, is bracketed by a composite transposon consisting of IS*Aba1* and transposases. *sul2, aph(3")lb, aph(6)-ld, and* bla_{NDM-1}, in B (shown as red arrows), were sandwiched between IS*1006*, recombinase, IS*Aba1*, IS*30*, and IS*Vsa3* insertion sequences and transposases.

Figure 3. Genetic environment of aph(3')-la, aac(3)-la, aadA1, sat2, dfrA, and Sat2 resistance genes on chromosomal contig 1 (~450-500kb, 2.04-2.06Mb, ~2.375-2.39Mb). IS*26*-IS*6* and IS*Ppu12* transposase bracketed *aph(3')-la*, *aac(3)-la*, and *aadA* while a recombinase and class 1 integron integrase (*IntI1*) sandwiched *sul1*, *qacE*, GNAT family N-acetyltransferase, and *aadA1* genes. Resistance genes are shown as blue arrows and mobile genetic elements are shown as red arrows. A DNA adenine methylase (purple arrow) was also found in close proximity to the resistance genes within the same genomic island on the chromosome (A). N-acetyl transferase and bla_{OXA-51} carbapenemase were also found in close proximity to *trmA* methylase (purple arrow) within the same region without any mobile genetic element (B). *dfrA*, *sat2*, and *aadA1* are also bracketed by a class 2 integron (*IntI2*), IS*256* and Tns*D/E* (Tn-*7*-like) transposases (C).

Figure 4. Genetic environment of aadA1, sat2, dfrA, and blaADC resistance genes on chromosomal contig 2 (0-15kb, 710-720kb, 1.8Mb-1.82Mb). IS256, Tns*E*, and tns*D* mobile genetic elements (shown in red arrows), recombinase (orange arrow), and an endonuclease (purple arrow) bracketed *dfrA*, *sat2*, *aadA (A)* while bla_{ADC} was in close synteny with IS*Aba1*

(B). The region shown in C is a "cut and paste" transposition of the region shown in A but in the reverse orientation, suggesting that a replicative transposition event occurred within the genome.

Figure 5. Genetic environment of mcr-1, tet(M), QnrS1, dfrA15, blaTEM-135, tet(A), cmlA1, aadA, qaC, and sul3 resistance genes on plasmid pR-B2.MM_C3 (contig 3). The resistance genes (blue arrows) were clustered together on a genomic island on pR-B2.MM_C3 at 0-42kb and 155kb-0kb and sandwiched between composite transposons (red arrows) and integrons (orange arrows). The mobile genetic environment comprised of composite transposons such as IS*903B,* IS*26,* IS*1380,* IS*1A, and* Tn*3,* alongside recombinases and class 1 *IntI1* integron. Site-specific DNA methylases were also found within this genomic island.

Figure 6. Phylogenetic analysis of antibiotic-resistant Acinetobacter baumannii strains from Africa. The R-B2.MM strain was not closely related to any resistant strain in Africa. The most closely related strains (*A. baumannii* 13259 and 13367) were not supported by the bootstrap values to be significant. The R-B2.MM strain is shown as red while all other strains are shown as black. Bootstrap values of ≥ 50 is significant. The resistomes of the three strains are also shown in a Table below the tree, with *A. baumannii* 13367 having more similarity with this study's strain. MLST (1) is the Pasteur Institute typing scheme while MLST (2) is the PubMLST typing scheme.

Figure 7. Phylogenetic analysis of antibiotic-resistant global Acinetobacter baumannii strains. *A. baumannii* Ab905 (from Tel-Aviv, Israel in 2019), Ab241 (from Tel-Aviv, Israel in 2019), Ab238 (from Tel-Aviv, Israel in 2019), AbCTX19 (from Le Kremlin Bicetre, France in 2019), and A3232 (Greece, 2022) strains formed the same clade with the R-52.MM strain. All these strains were isolated from humans and mostly from blood except strain AbCTX19 (rectal swab). Ab241 and Ab238 were of the same MLST (106 or 3) while AbCTX19 and A3232 were of MLST 231 (and 1 or 160, respectively). The significance of the clade was confirmed by the bootstrap. A3232 was most closely related to R-B2.MM evolutionarily and is thus shown as red on the tree. Bootstrap values of ≥ 50 is significant. MLST (1) is the Pasteur Institute typing scheme while MLST (2) is the PubMLST typing scheme.

Figure 8. A volcano plot showing differentially expressed genes (DEGs) in Acinetobacter baumannii R-B2.MM exposed to colistin and carbapenems. The significant DEGs are

shown in red while the non-significant DEGs are shown in grey. The significant DEGs include genes within the category of hypothetical protein, LysR transcriptional regulator, phage replication protein, aliphatic sulfonate monooxygenase, aldehyde dehydrogenase. Putative lipoprotein, urea carboxylase-related aminomethyltransferase, ribulose-5-phosphate 4-epimerase, and VgrG protein.

Supplemental Tables

Supplemental dataset 1. Datasets comprising of Tables S1 (mcr primers), S2 (antimicrobial sensitivity testing, AST, MIC results), S3 (resistome), S4 (colistin-efflux pump inhibitors results), and S5 (carbapenem-efflux pump inhibitors results).

Supplemental dataset 2. Datasets comprising of metadata on demographics, clones (STs), biosamples, country of isolation, year and source of isolation, and resistance genes of strains from Africa and Globally.

Supplemental dataset 3. Datasets of Tables showing differentially expressed or repressed genes of Acinetobacter baumannii R-B2.MM.

Supplemental dataset 4. Datasets on methylation data, methylases, and DNA methylation motifs.

Supplemental Figures

Figure S1. Genetic environment of resistance genes found on a genomic island on a chromosome (contig 1: 0kb to 85kb). All the resistance genes (shown in blue) were bracketed by mobile genetic elements (shown in red and orange) and clustered together on the island. The close alignment of this region with other plasmids and chromosomes show that this region was a plasmid that was integrated into the chromosome. Epigenomically, DNA methyltransferases and methylase were also found within the genomic island.

Figure S2. Genetic environment of resistance genes found on contig 1 (between 0kb to 40kb) shows mobile genetic elements bracketing the resistance genes. This image is an expansion of Figure S1 between the 0 - 40kb region above.

Figure S3. Genetic environment of resistance genes found on contig 1(between 40kb to 80kb) shows mobile genetic elements bracketing the resistance genes. This image is an expansion of Figure S1 between the 40 - 80kb region above.

Figure S4. Genetic environment of resistance genes found on contig 1 (~135kb-180kb) shows mobile genetic elements bracketing the resistance genes. This image is based on the region between 130kb and180kb, showing a methyltransferase to epigenetic gene regulation. *gyr*B, which can confer resistance to fluoroquinolones when there are mutations, was found in this region without any MGE around it.

Figure S5. Mobile genetic elements and methyltransferases on contig 1 between 120kb to 250kb region. This region harbours methyltransferases, gyrB, and an ISAba1 mobile genetic element.

Figure S6. Genetic environment of resistance genes found on plasmid pR-B2.MM_C3. The plasmid contains methyltransferases, composite transposons, and integrons bracketing the resistance genes, which were clustered together within a genomic island surrounded by mobile genetic elements such as integrons, composite transposons, and insertion sequences.

Figure S7. Genetic map of pR-B2.MM_C6. A circularized map of pR-B2.MM_C6. pR-B2.MM_C6 has no resistance gene.

Figure S8. Top functional categories of significantly and differentially expressed genes (DEGs) in isolate R-B2.MM. Most of the DEGs belonged to hypothetical proteins with no known function, transcriptional regulators, and mobile genetic elements.

Figure S9. Phylogenetic analysis of antibiotic-resistant global Acinetobacter baumannii strains with close sequence homology to R-B2.MM. A. baumannii strains that had close sequence homology to R-B2.MM after nucleotide BLAST showed very close evolutionary association with the R-B2.MM. The strains with very close evolutionary association to the R-B2.MM strain are shown as blue text in A. The resistome is shown in B. The resistome were not conserved across the strains on the same clade. Resistance genes that were conserved across the species includes the $bla_{OXA\text{-}69}$ and bla_{ADC}.

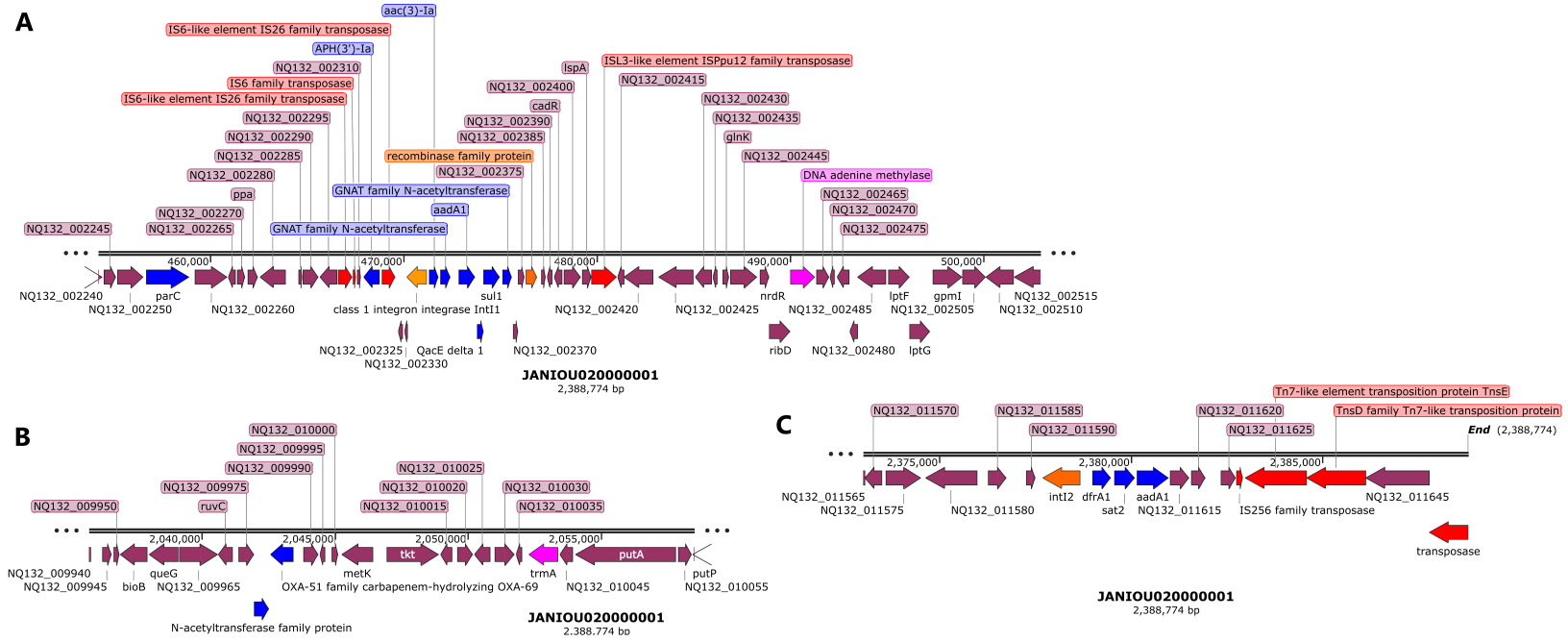
A
aac(3)-Ia
IS6-like element IS26 family transposase
APH(3')-Ia
NQ132_002310
IS6 family transposase
IS6-like element IS26 family transposase
NQ132_002295
NQ132_002290
NQ132_002285
NQ132_002280
ppa
NQ132_002270
NQ132_002245
NQ132_002265
GNAT family N-acetyltransferase
recombinase family protein
NQ132_002375
GNAT family N-acetyltransferase
aadA1
lspA
ISL3-like element ISPpu12 family transposase
NQ132_002400
NQ132_002415
cadR
NQ132_002390
NQ132_002385
NQ132_002430
NQ132_002435
glnK
NQ132_002445
DNA adenine methylase
NQ132_002465
NQ132_002470
NQ132_002475
460,000
470,000
480,000
490,000
500,000
NQ132_002240
parC
NQ132_002250
NQ132_002260
class 1 integron integrase IntI1
sul1
NQ132_002420
NQ132_002425
nrdR
NQ132_002485
lptF
gpmI
NQ132_002505
NQ132_002515
NQ132_002510
NQ132_002325
QacE delta 1
NQ132_002330
NQ132_002370
ribD
NQ132_002480
lptG
JANIOU020000001
2,388,774 bp
B
NQ132_010000
NQ132_009995
NQ132_009990
NQ132_009975
NQ132_009950
ruvC
NQ132_010025
NQ132_010020
NQ132_010015
NQ132_010030
NQ132_010035
2,040,000
2,045,000
2,050,000
2,055,000
tkt
putA
NQ132_009940
NQ132_009945
queG
bioB
NQ132_009965
metK
OXA-51 family carbapenem-hydrolyzing OXA-69
trmA
NQ132_010045
putP
NQ132_010055
N-acetyltransferase family protein
JANIOU020000001
2.388.774 bo
C
Tn7-like element transposition protein TnsE
NQ132_011570
NQ132_011585
NQ132_011620
TnsD family Tn7-like transposition protein
NQ132_011590
NQ132_011625
End (2,388,774)
2,375,000
2,380,000
2,385,000
NQ132_011565
NQ132_011575
NQ132_011580
intI2
dfrA1
sat2
aadA1
NQ132_011615
IS256 family transposase
NQ132_011645
transposase
JANIOU020000001
2,388,774 bp

A

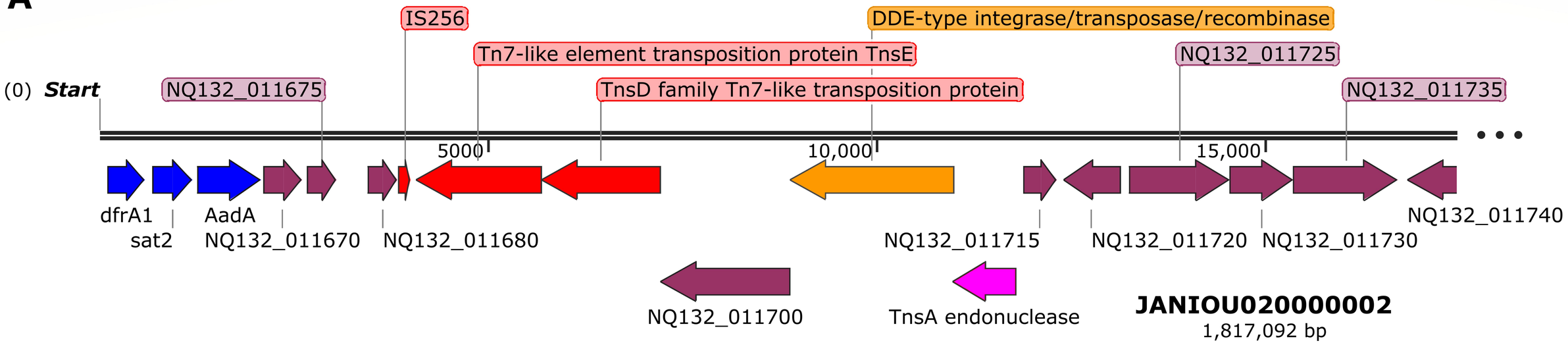
IS256
DDE-type integrase/transposase/recombinase
Tn7-like element transposition protein TnsE
NQ132_011725
(0) Start
NQ132_011675
TnsD family Tn7-like transposition protein
NQ132_011735
5000
10,000
15,000
dfrA1
sat2
AadA
NQ132_011670
NQ132_011680
NQ132_011740
NQ132_011715
NQ132_011720
NQ132_011730
NQ132_011700
TnsA endonuclease
JANIOU020000002
1,817,092 bp

B

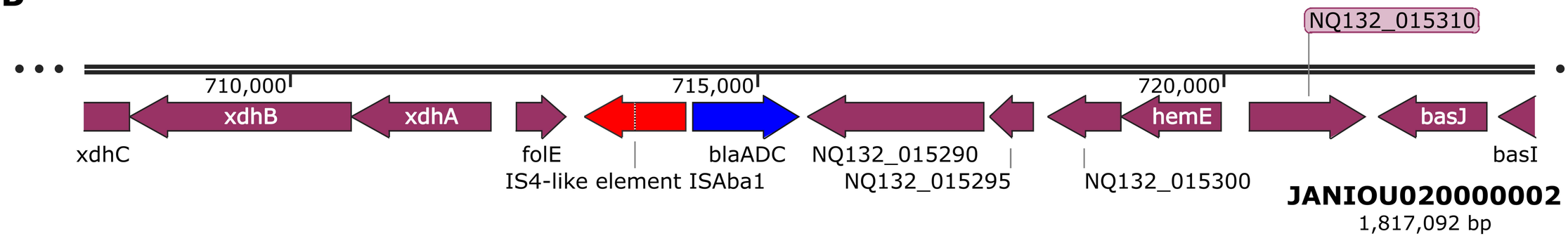
NQ132_015310
710,000
715,000
720,000
xdhB
xdhA
hemE
basJ
xdhC
folE
blaADC
NQ132_015290
basI
IS4-like element ISAba1
NQ132_015295
NQ132_015300
JANIOU020000002
1,817,092 bp

C

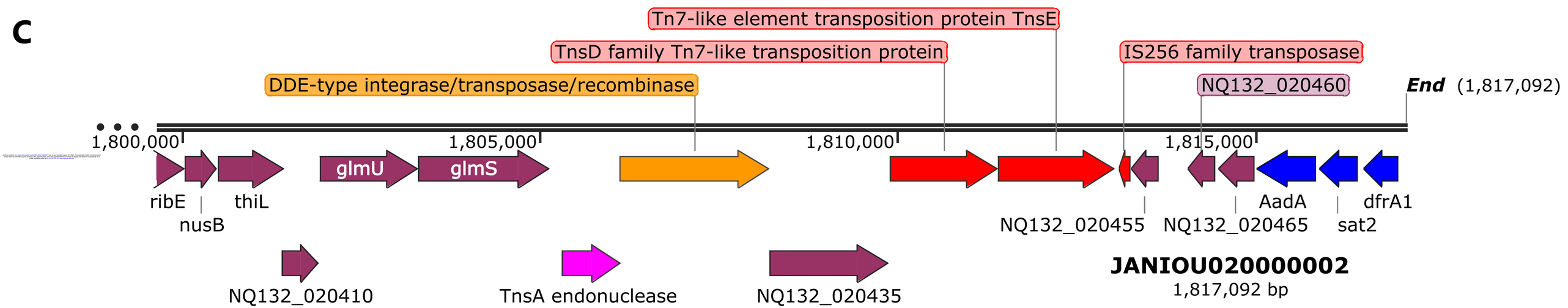
Tn7-like element transposition protein TnsE
TnsD family Tn7-like transposition protein
IS256 family transposase
DDE-type integrase/transposase/recombinase
NQ132_020460
End (1,817,092)
1,800,000
1,805,000
1,810,000
1,815,000
glmU
glmS
ribE
nusB
thiL
AadA
dfrA1
sat2
NQ132_020455
NQ132_020465
NQ132_020410
TnsA endonuclease
NQ132_020435
JANIOU020000002
1,817,092 bp

A

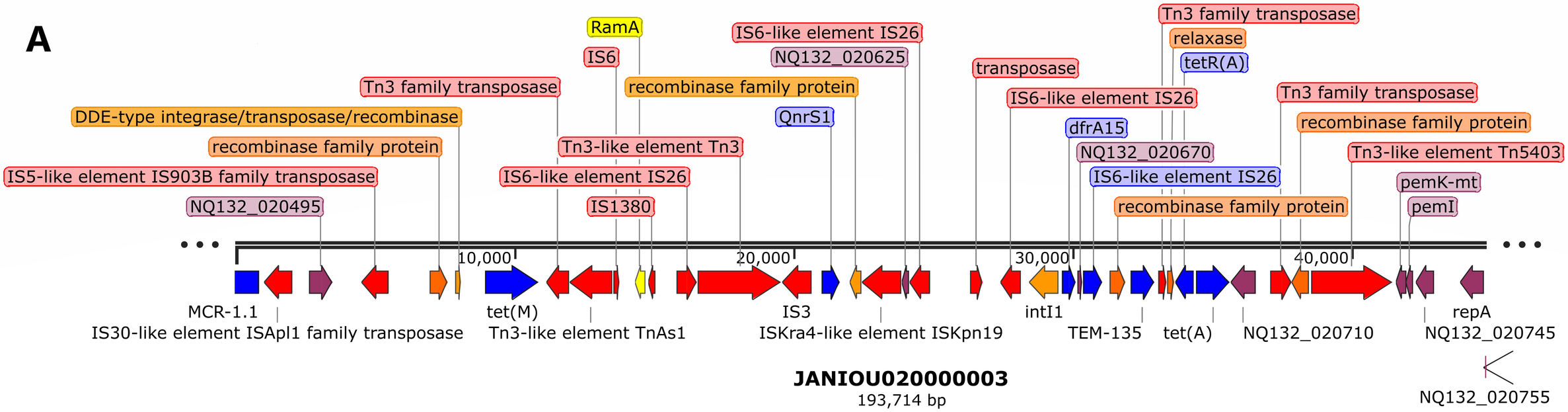
RamA
IS6
IS6-like element IS26
NQ132_020625
Tn3 family transposase
relaxase
tetR(A)
transposase
Tn3 family transposase
recombinase family protein
IS6-like element IS26
DDE-type integrase/transposase/recombinase
QnrS1
dfrA15
recombinase family protein
Tn3-like element Tn3
NQ132_020670
Tn3-like element Tn5403
IS5-like element IS903B family transposase
IS6-like element IS26
IS6-like element IS26
pemK-mt
NQ132_020495
IS1380
recombinase family protein
pemI
10,000
20,000
30,000
40,000
MCR-1.1
IS30-like element ISApl1 family transposase
tet(M)
Tn3-like element TnAs1
IS3
ISKra4-like element ISKpn19
intI1
TEM-135
tet(A)
NQ132_020710
repA
NQ132_020745
NQ132_020755
JANIOU020000003
193,714 bp

B

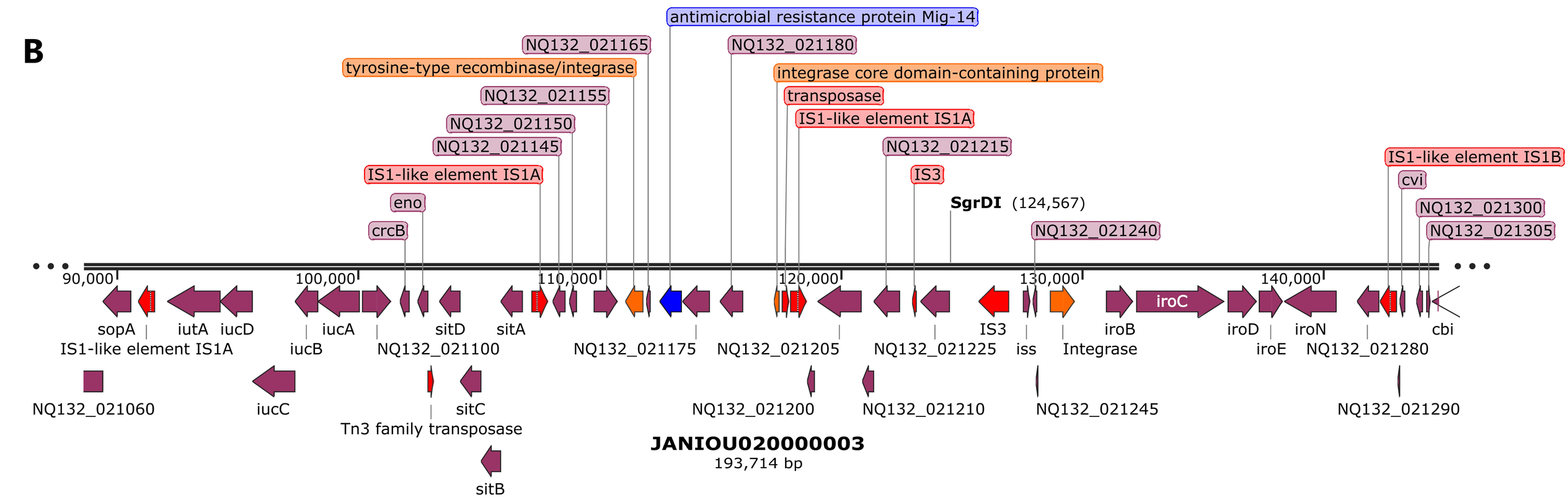
antimicrobial resistance protein Mig-14
NQ132_021165
NQ132_021180
tyrosine-type recombinase/integrase
integrase core domain-containing protein
NQ132_021155
transposase
NQ132_021150
IS1-like element IS1A
NQ132_021145
NQ132_021215
IS1-like element IS1B
IS1-like element IS1A
IS3
cvi
eno
SgrDI (124,567)
NQ132_021300
crcB
NQ132_021240
NQ132_021305
90,000
100,000
110,000
120,000
130,000
140,000
iroC
sopA
iutA
iucD
iucA
sitD
sitA
IS3
iroB
iroD
iroN
cbi
IS1-like element IS1A
iucB
NQ132_021100
NQ132_021175
NQ132_021205
NQ132_021225
iss
Integrase
iroE
NQ132_021280
NQ132_021060
iucC
sitC
NQ132_021200
NQ132_021210
NQ132_021245
NQ132_021290
Tn3 family transposase
sitB
JANIOU020000003
193,714 bp

C

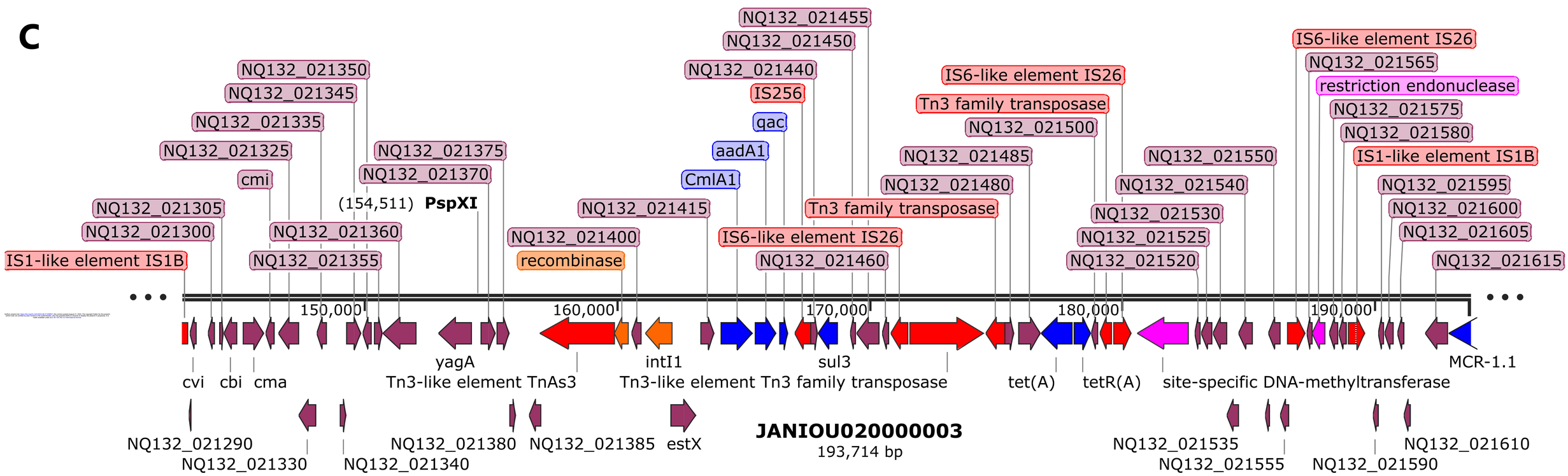
NQ132_021455
NQ132_021450
IS6-like element IS26
NQ132_021565
NQ132_021350
NQ132_021440
IS6-like element IS26
restriction endonuclease
NQ132_021345
IS256
Tn3 family transposase
NQ132_021575
NQ132_021335
qac
NQ132_021500
NQ132_021580
NQ132_021325
aadA1
NQ132_021375
NQ132_021485
NQ132_021550
IS1-like element IS1B
cmi
CmlA1
NQ132_021370
NQ132_021480
NQ132_021540
NQ132_021595
(154,511) PspXI
NQ132_021415
Tn3 family transposase
NQ132_021530
NQ132_021600
NQ132_021305
NQ132_021300
NQ132_021360
NQ132_021400
IS6-like element IS26
NQ132_021525
NQ132_021605
IS1-like element IS1B
NQ132_021355
recombinase
NQ132_021460
NQ132_021520
NQ132_021615
150,000
160,000
170,000
180,000
190,000
cvi
cbi
cma
yagA
Tn3-like element TnAs3
intI1
Tn3-like element Tn3 family transposase
sul3
tet(A)
tetR(A)
site-specific DNA-methyltransferase
MCR-1.1
NQ132_021290
NQ132_021330
NQ132_021340
NQ132_021380
NQ132_021385
estX
JANIOU020000003
193,714 bp
NQ132_021535
NQ132_021555
NQ132_021590
NQ132_021610

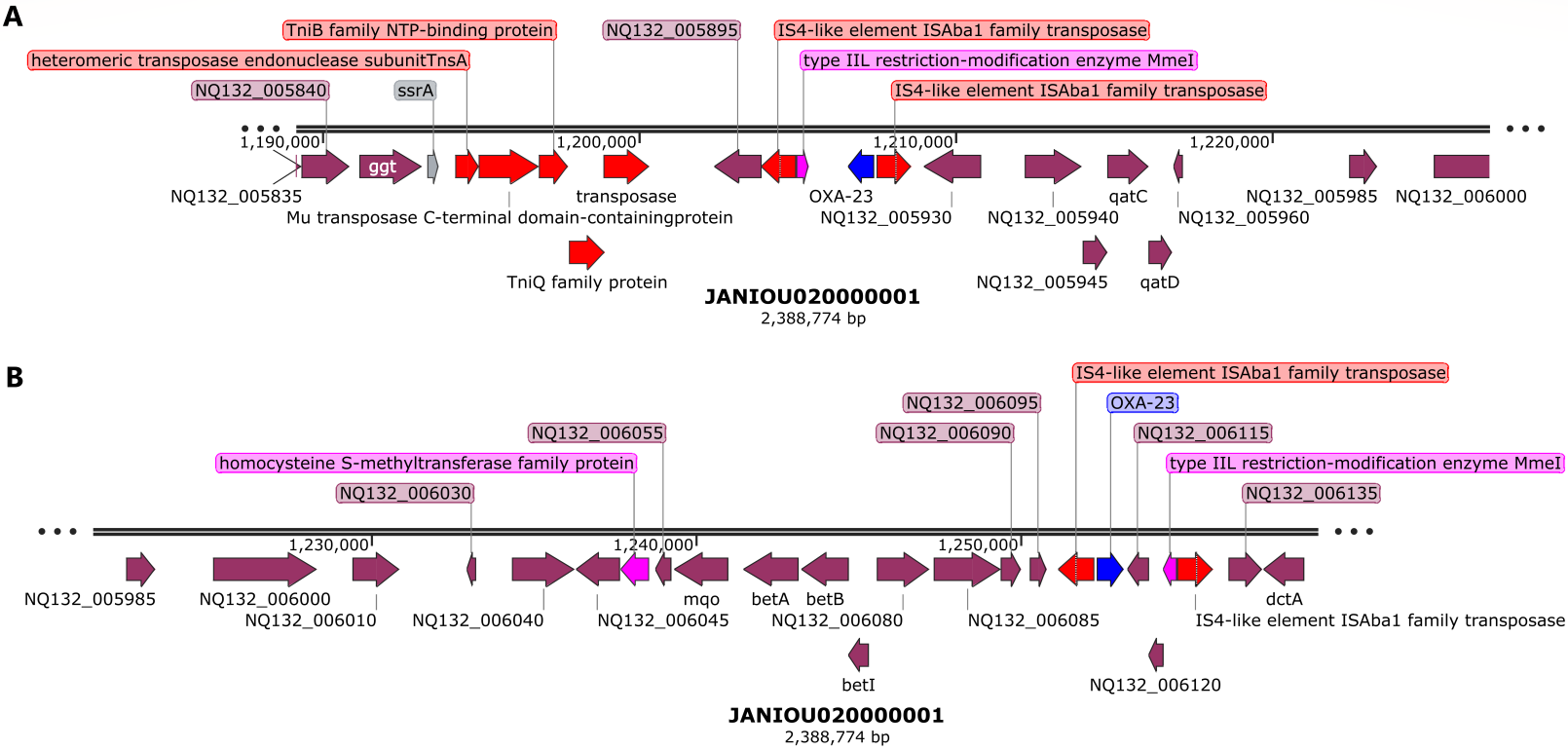
A
TniB family NTP-binding protein
NQ132_005895
IS4-like element ISAba1 family transposase
heteromeric transposase endonuclease subunitTnsA
type IIL restriction-modification enzyme MmeI
NQ132_005840
ssrA
IS4-like element ISAba1 family transposase
1,190,000
1,200,000
1,210,000
1,220,000
ggt
NQ132_005835
Mu transposase C-terminal domain-containingprotein
transposase
OXA-23
NQ132_005930
NQ132_005940
qatC
NQ132_005960
NQ132_005985
NQ132_006000
TniQ family protein
NQ132_005945
qatD
JANIOU020000001
2,388,774 bp
B
IS4-like element ISAba1 family transposase
NQ132_006095
OXA-23
NQ132_006055
NQ132_006090
NQ132_006115
homocysteine S-methyltransferase family protein
type IIL restriction-modification enzyme MmeI
NQ132_006030
NQ132_006135
1,230,000
1,240,000
1,250,000
NQ132_005985
NQ132_006000
NQ132_006010
NQ132_006040
NQ132_006045
mqo
betA
betB
NQ132_006080
NQ132_006085
dctA
IS4-like element ISAba1 family transposase
betI
NQ132_006120
JANIOU020000001
2,388,774 bp

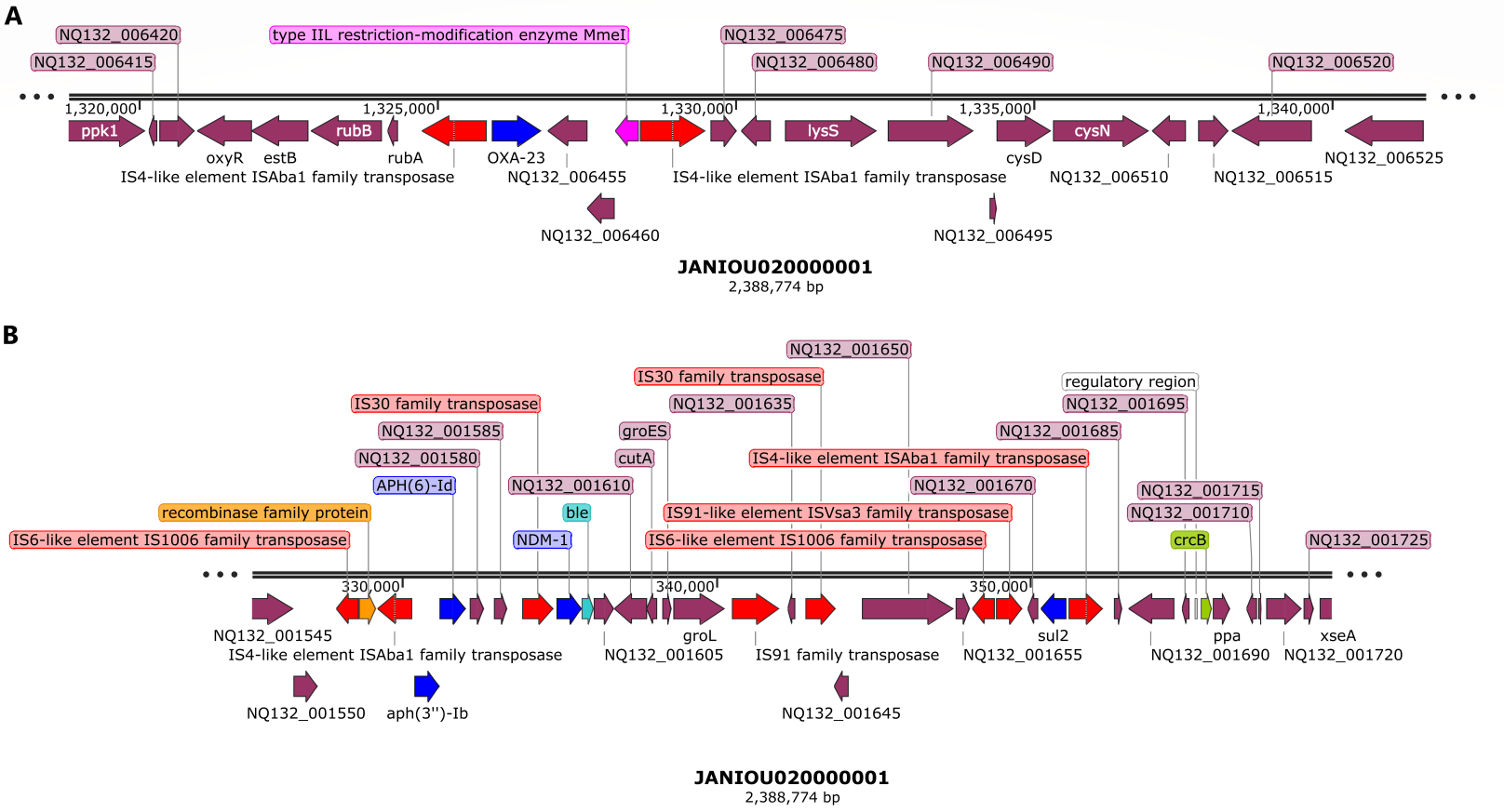
A
NQ132_006420
NQ132_006415
type IIL restriction-modification enzyme MmeI
NQ132_006475
NQ132_006480
NQ132_006490
NQ132_006520
1,320,000
1,325,000
1,330,000
1,335,000
1,340,000
ppk1
oxyR
estB
rubB
rubA
OXA-23
lysS
cysD
cysN
NQ132_006525
IS4-like element ISAba1 family transposase
NQ132_006455
IS4-like element ISAba1 family transposase
NQ132_006510
NQ132_006515
NQ132_006460
NQ132_006495
JANIOU020000001
2,388,774 bp
B
NQ132_001650
IS30 family transposase
regulatory region
IS30 family transposase
NQ132_001635
NQ132_001695
NQ132_001585
groES
NQ132_001685
NQ132_001580
cutA
IS4-like element ISAba1 family transposase
APH(6)-Id
NQ132_001610
NQ132_001670
NQ132_001715
recombinase family protein
ble
IS91-like element ISVsa3 family transposase
NQ132_001710
IS6-like element IS1006 family transposase
NDM-1
IS6-like element IS1006 family transposase
crcB
NQ132_001725
330,000
340,000
350,000
NQ132_001545
IS4-like element ISAba1 family transposase
groL
NQ132_001605
IS91 family transposase
sul2
NQ132_001655
ppa
NQ132_001690
xseA
NQ132_001720
NQ132_001550
aph(3'')-Ib
NQ132_001645
JANIOU020000001
2,388,774 bp

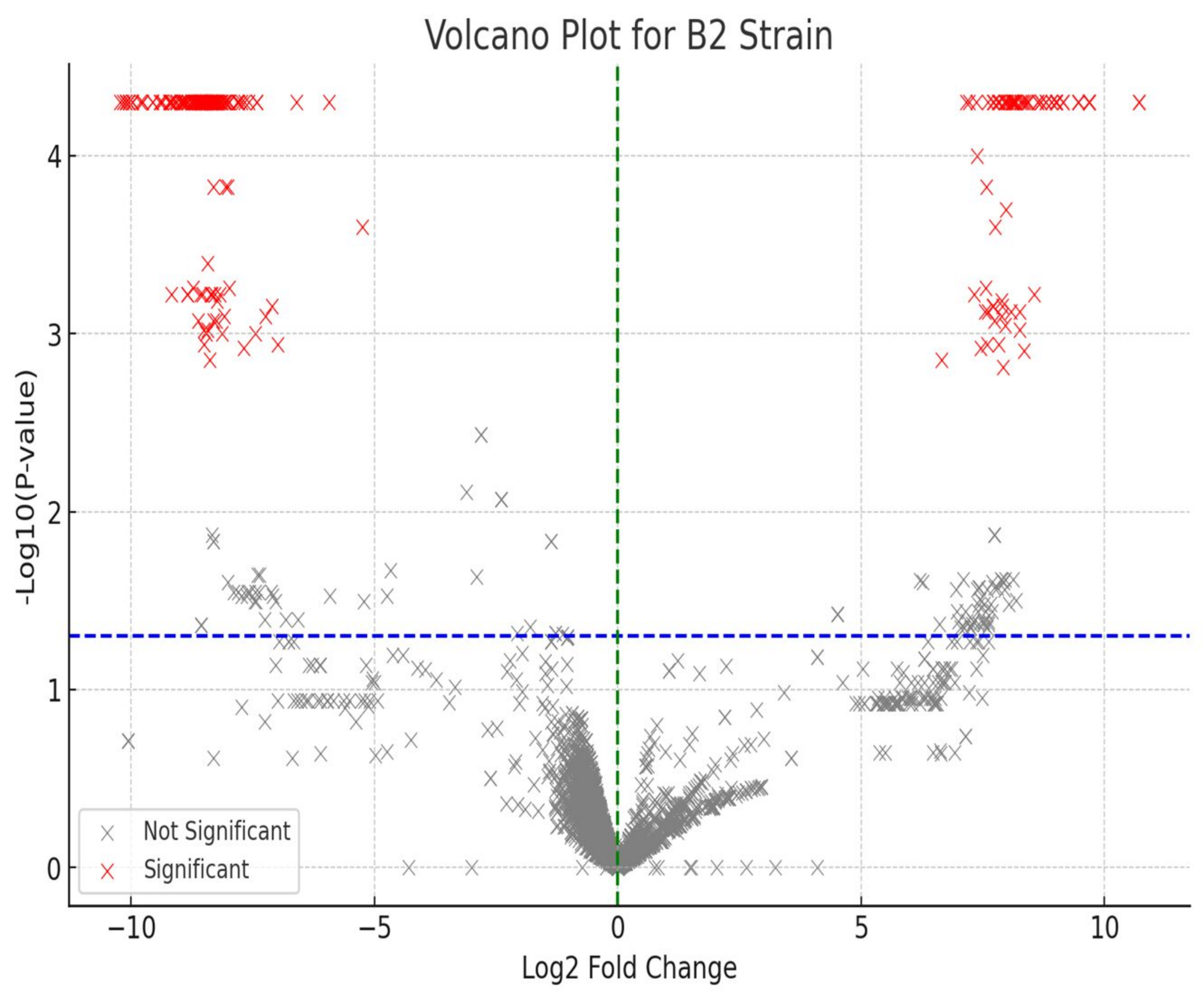
Volcano Plot for B2 Strain
-Log10(P-value)
Log2 Fold Change
Not Significant
Significant
4
3
2
1
0
−10
−5
0
5
10

A

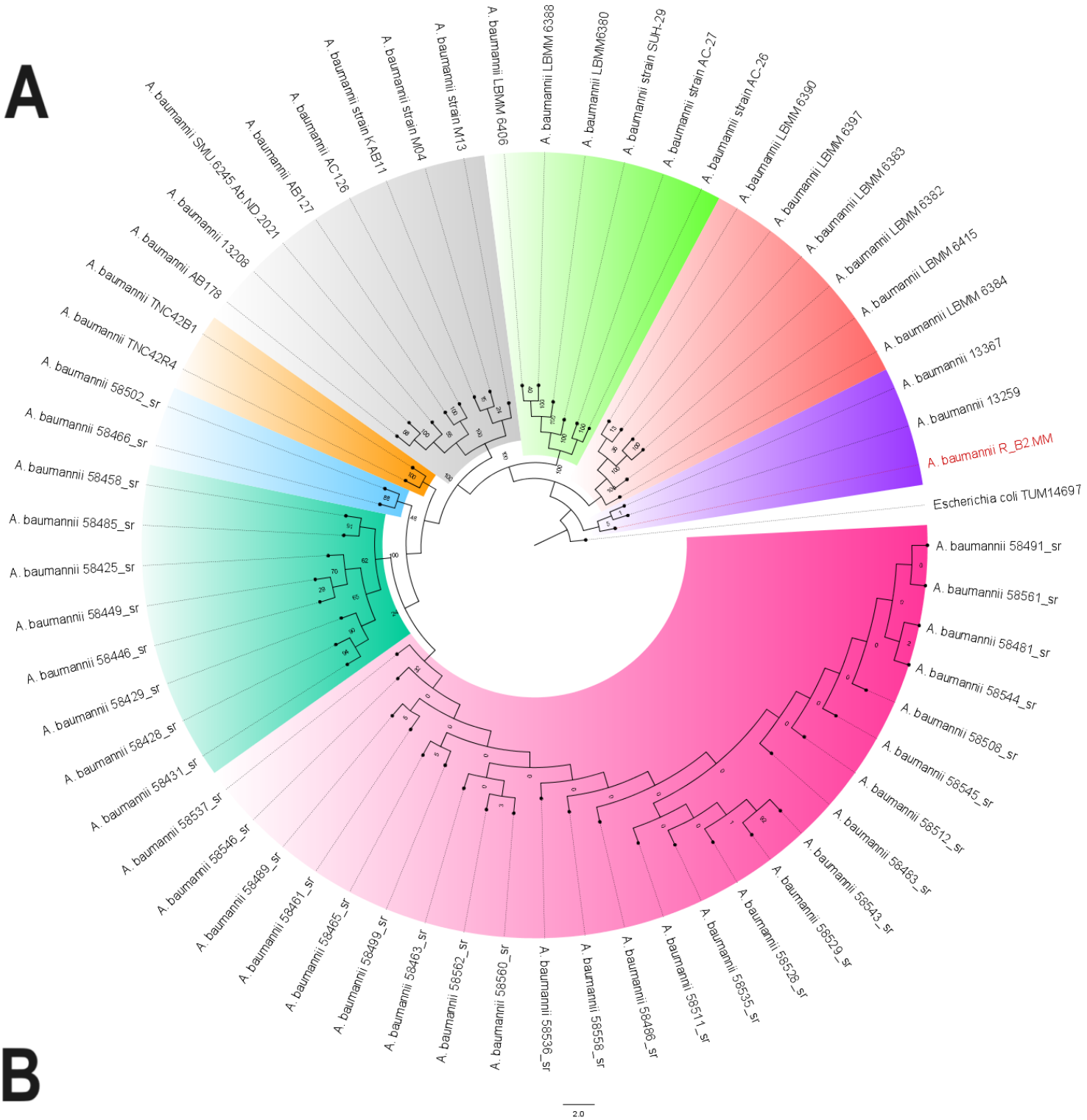

B

Genome Name	MLST	Isolation Source	Collection Date	Location	Host	Host Health	abaF	aac(3)-Ia	amvA	aadA1	ant(2'')-Ia	ant(3'')-IIa	aph(3'')-Ib	aph(3')-Ia	aph(3')-VIa	aph(6)-Id	armA
A. baumannii 13367	(1)339	Blood culture	2018-05-06	South Africa	Human	Neonatal sepsis	abaF		amvA		ant(2'')-Ia	ant(3'')-IIa	aph(3'')-Ib		aph(3')-VIa	aph(6)-Id	
A. baumannii 13259	(2)243	Blood culture	2018-03-26	South Africa	Human	Neonatal sepsis	abaF		amvA		ant(2'')-Ia	ant(3'')-IIa			aph(3')-VIa		
A. baumannii R-B2.MM	(1)1, (2)231, 1604	Fluid aspirate	2017	South Africa	Human			aac(3)-Ia		aadA1			aph(3'')-Ib	aph(3')-Ia		aph(6)-Id	armA

Genome Name	blaADC	blaPER	blaOXA-58	blaOXA-23	blaNDM-1	blaOXA	arr-2	gyrA_S81L	blaTEM-1	sul2	sul1	sul3	mcr-1	cmlA5	mph(E)	dfrA	msr(E)	floR	tet(A)	tet(B)	tet(M)	qnrS1
A. baumannii 13367	blaADC-87			blaOXA-23		blaOXA	arr-2			sul2	sul1			cmlA5	mph(E)	dfrA23/45	msr(E)	floR		tet(B)		
A. baumannii 13259	blaADC		blaOXA-58			blaOXA		gyrA_S81L		sul2												
A. baumannii R-B2.MM	blaADC-25	blaPER-7	blaOXA-69	blaOXA-23	blaNDM-1		arr-2		blaTEM-1B	sul2	sul1	sul3	mcr-1.cmlA1		mph(E)	dfrA1/15	msr(E)		tet(A)	tet(B)	tet(M)	qnrS1

A

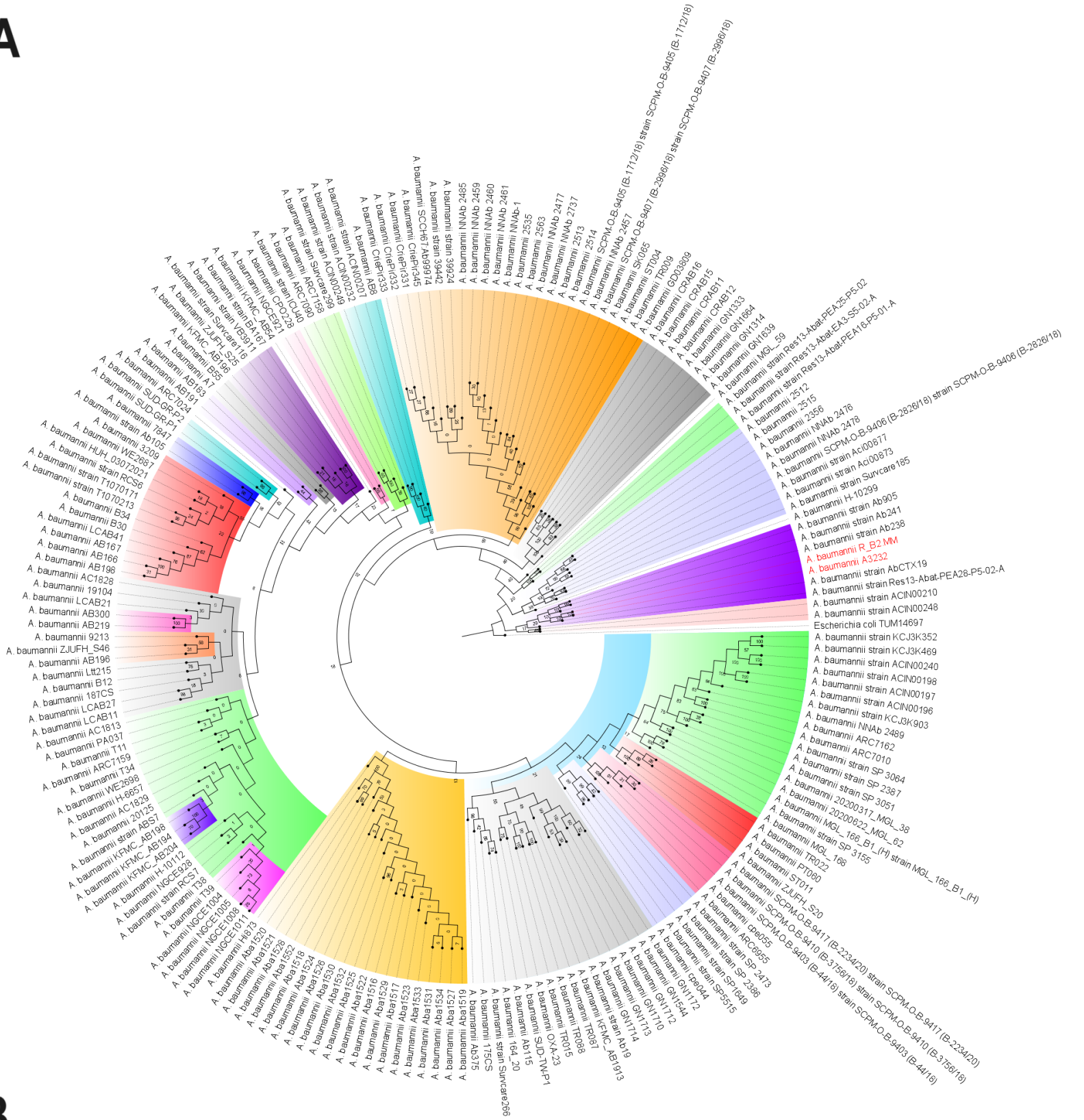

B

Genome Name	MLST	Isolation Source	Collection Date	Location	Host	Host Health	abaF	aac(3)-Ia	amvA	aadA1	aph(3'')-Ib	aph(3')-Ia	adeC	ant(3'')-IIa	ant(2'')-Ia	aph(6)-Id	aph(3')-VIa	armA	blaADC	blaPER	blaOXA-58	blaOXA-23	blaNDM-1
A. baumannii Ab905		blood	2019-01	Israel:Tel-Aviv	Human	A. baumannii	abaF		amvA				adeC	ant(3'')-IIa	ant(2'')-Ia				blaADC-263		blaOXA-71	blaOXA-23	
A. baumannii Ab241	(1)106, (2)3	blood	2019-01	Israel:Tel-Aviv	Human	A. baumannii	abaF		amvA				adeC	ant(3'')-IIa	ant(2'')-Ia		aph(3')-VIa		blaADC-263		blaOXA-71	blaOXA-23	
A. baumannii SP 2387	(2)2	Respiratory specimen	2020	India: Vellore	Human	Pnuemonia																	
A. baumannii A3232	(2)160, (1)231	blood	2022-12-23	Greece	Human	Not known	abaF	aac(3)-Ia	amvA	aadA1	aph(3'')-Ib	aph(3')-Ia	adeC	ant(3'')-IIa		aph(6)-Id	aph(3')-VIa		blaADC-191			blaOXA-23	blaNDM-1
A. baumannii AbCTX19	(2)1 (1)231	Rectal swab	2019-11	France	Human	Colonization	abaF		amvA	aadA5			adeC	ant(3'')-IIa			aph(3')-VIa	armA	blaADC-30		blaOXA-72		
A. baumannii R-B2.MM	(1)1, (2)231, 1604	Fluid aspirate	2017	South Africa	Human			aac(3)-Ia		aadA1	aph(3'')-Ib	aph(3')-Ia				aph(6)-Id		armA	blaADC-25	blaPER-7	blaOXA-69	blaOXA-23	blaNDM-1

Genome Name	blaOXA	arr-2	gyrA_S81L	parC_S84L	blaTEM-1	sul2	sul1	sul3	mcr-1	cmlA5	catA1	mph(E)	dfrA	msr(E)	floR	tet(A)	tet(B)	tet(M)	qnrS1	blaCTX-M-115	ble	sat2
A. baumannii Ab905			gyrA_S81L	parC_S84L			sul1									tet(A)						
A. baumannii Ab241			gyrA_S81L	parC_S84L			sul1									tet(A)						
A. baumannii SP 2387																						
A. baumannii A3232	blaOXA-69		gyrA_S81L			sul2	sul1						dfrA1				tet(B)				ble	sat2
A. baumannii AbCTX19	blaOXA-69		gyrA_S81L			sul2	sul1				catA1	mph(E)		msr(E)	floR					blaCTX-M-115		
A. baumannii R-B2.MM		arr-2			blaTEM-1B	sul2	sul1	sul3	mcr-1.1	cmlA1		mph(E)	dfrA1/15	msr(E)		tet(A)	tet(B)	tet(M)	qnrS1			